Design and fabrication of sinusoidal filters for multispectral imaging

Chuan Ni*, Jie Jia, Keigo Hirakawa, Andrew Sarangan
Electro-Optics Graduate Program, University of Dayton, 300 College Park, Dayton, OH, USA 45469-2951

ABSTRACT

Multispectral imaging beyond the three RGB colors still remains a challenge, especially in portable inexpensive systems. In this paper, we describe the design and fabrication of broadband multichroic filters that have a sinusoidal transmission spectra to utilize a novel methodology based on the Fourier spectral reconstruction in the frequency domain. Since the spectral filters are posed as an optimal sampling of hyperspectral images, they also allow for the reconstruction of the full spectrum from subsequent demosaicking algorithms.

Unlike conventional Color Filter Arrays (CFA) which utilizes absorption dyes embedded in a polymeric material, the sinusoidal multichroic filters require an all-dielectric interference filter design. However, the goal of most dielectric filter designs is to achieve sharp transitions with high-contrast. A smoothly varying sinusoidal transition is more difficult with conventional approaches. However, this can be achieved by trading off the contrast. Following the principles of a simple Fabry-Perot cavity, we have designed and built interference filters from 0.5 sinusoidal periods to 3 sinusoidal periods from 450nm to 900nm spectral range. Also, in order to maintain a uniform period across the entire spectrum, the material must have a very low dispersion. In this design, we have used ZnS as the cavity material. The six filters have been used in a multispectral imaging test bed.

Keywords: multispectral imaging, Fabry-Perot cavity, spectral filter array

1. INTRODUCTION

Conventional cameras that use color filter arrays (CFAs) only capture the basic RGB color information which perform the retrieval of relative color information, but are not able to identify objects or perform a more complete spectral analysis [1]. Multispectral imaging requires significantly more spectral information beyond these three broad spectral bands to enable chemical and material identification, and for improving the accuracy of object recognition. However, the acquisition of multispectral data still remains a challenge in many applications, especially when the end application requires portable inexpensive systems.

The conventional approach for multispectral imaging is based on using narrowband spectral filters [2,3]. Such imaging systems are optimized for a predetermined set of wavelengths for detecting the presence or absence of those emissions from the objects. Examples include biomedical imaging and astronomy. As such, they cannot be easily adapted for different applications because it would require changing the entire filter set.

In this work, we are utilizing an innovative methodology with an array of broadband multichroic filters that have a sinusoidal transmission spectrum in the frequency domain, also known as the Fourier filters. These broadband filters are able to capture a wider range of spectral content compared to narrow band filters, especially for the same number of filter elements.

*cni001@udayton.edu

2. FOURIER SPECTRAL FILTERS

Design of Fourier Spectral Filters

The Fourier spectral filters' transmission spectra are shown in Figure 1. The design algorithm of these filters is discussed in greater detail in [4]. Each filter contains an increasing number of sinusoid in the spectral domain. Note that these were designed to be sinusoids in the frequency domain, hence they appear skewed when plotted in the wavelength domain.

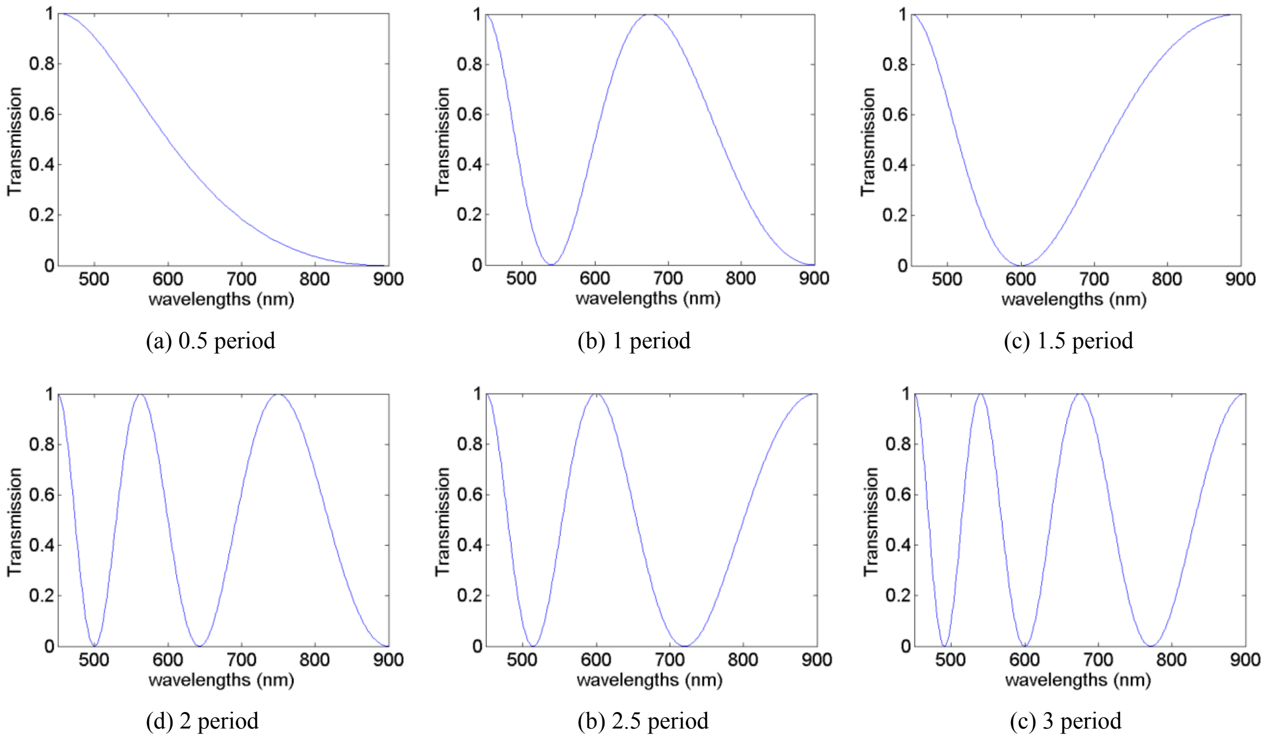

(a) 0.5 period (b) 1 period (c) 1.5 period

(d) 2 period (b) 2.5 period (c) 3 period

Figure 1. Expected Fourier spectral filters transmission.

Unlike most dielectric filters, which are designed to provide sharp transitions with high contrast - such as high-pass, low-pass, band-pass, etc., - a smoothly varying sinusoidal transition is much more difficult to achieve with established thin film design methodologies. There aren't many applications that require filters with smooth roll offs. Nevertheless, considering the periodic nature of the required spectra, one could potentially use a simple Fabry-Perot resonator the fundamental building block for this design. However, the transmission spectra of typical Fabry-Perot resonators are not sinusoidal; they contain a series of sharp high-transmission peaks surrounded by broad high-reflection bands. The narrow widths of the transmission peaks and the reflectivities are determined primarily by the termination reflectivites on each side of Fabry-Perot cavity, which is also described by the finesse factor of the cavity. As a result, only a very narrow spectral band near the resonance wavelength will be transmitted through the cavity, while all the other wavelengths are reflected back. The physical thickness of the cavity length, or spacer layer, determines the periodicity of the spectrum. Assuming normal incidence, the termination reflectivities dictate the minimum transmission between the peak values, viz. they dictate the contrast between the filter's maximum and minimum transmission points. By decreasing the termination reflectivities, finesse factor drops, and the transmission peaks start to broaden out and become smoother. By carefully adjusting the termination reflectivities, the transmission spectra can be made to closely approximate a sinusoidal function. In addition, material dispersion (change in refractive index as a function of wavelength) also plays an important role in the periodicity of the transmission peaks. A material with a low-dispersion property will be ideal to get a closest fit to a sinusoid across the entire spectral range of interest.

Comparing the designed Fabry-Perot filter to the perfect sinusoidal filter, we can define an error function to indicate the deviation of the Fabry-Perot filter from a perfect sinusoidal function. In the visible wavelength range from 450 nm to 900 nm, this error is accumulated by the difference between these two functions at each wavelength.

Assuming silica glass as the substrate and air as the medium above the film, we can sweep the refractive index of the Fabry-Perot cavity to compute the transmissions and reflections on both sides of layer and then describe the error as a function of the filter contrast. The transmission spectrum approaches a perfect sinusoid when the contrast drops to zero, which coincides with the refractive index of the cavity becoming equal to the substrate refractive index. Therefore, there is a trade-off between the filter contrast and the sinusoidal fit.

For this work, we used ZnS as the cavity spacer material. This is a widely used optical material and it is relatively easy to deposit by sputter processes, and has a relatively high refractive index around 2.35 in the visible spectrum. The corresponding reflectivities on each side of cavity are 16% on air side and 5% on the substrate side. The peak-to-valley contrast of the transmission spectrum is 28.8%, and the error between the ideal sinusoid and the Fabry-Perot transmission spectrum can be calculated to be 1.6%. Other materials such as TiO_2 have an even higher refractive index in the visible, and can provide a larger contrast, but they also suffer from greater dispersion resulting in a larger deviation from the ideal sinusoid. Al_2O_3, on the other hand, has a much smaller dispersion in the desired wavelength range (refractive index change less than 0.05 in visible), but its contrast is significantly smaller due to the lower refractive index around 1.75. The refractive index dispersion data were measured and fitted by a spectrometer and is shown in Figure 2(a). The one-period sinusoidal transmission spectra by using these three materials were simulated and are shown in Figure 2(b). Therefore, it can be seen that ZnS provides a reasonable compromise between performance and deviation from the ideal spectral shape.

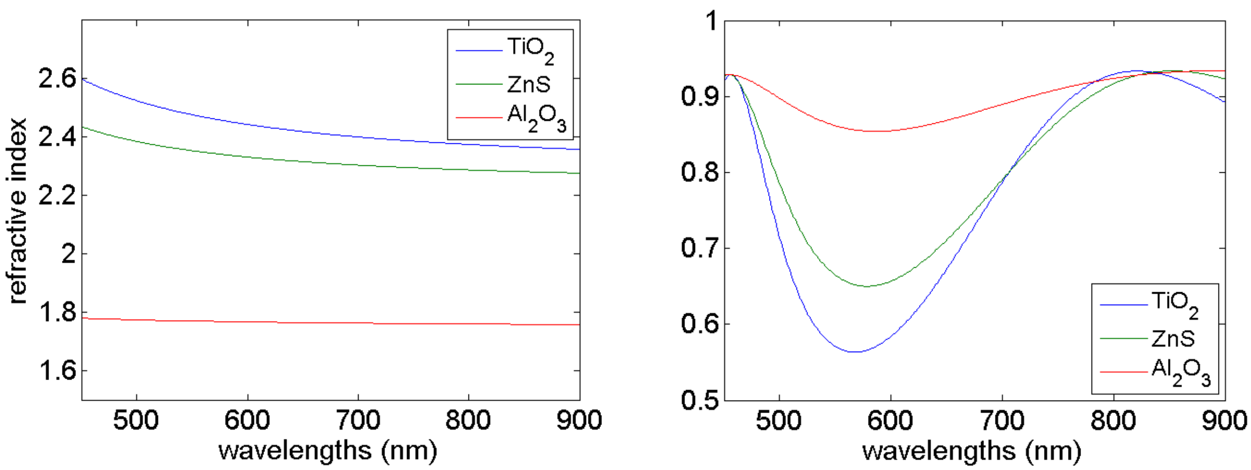

(a) Refractive indices

(b) one-period sinusoid transmission spectra

Figure 2. Material comparison: TiO_2, ZnS and Al_2O_3.

By changing the cavity thickness, we are able to produce filters with different sinusoidal transmission spectra. For example, half a sinusoidal oscillation between 450 nm and 900 nm can be obtained with a ZnS thickness of 96 nm. Two sinusoidal oscillations can be obtained with a thickness of 390 nm, and three oscillations can be obtained with a thickness of 560 nm.

Fabrication of Fourier Spectral Filters

We used RF sputter deposition to fabricate all the filters. Sputter deposition is more suitable for ZnS compared with other thin film deposition techniques like evaporation or chemical vapor deposition. Evaporation can lead to dissociation of zinc and sulfur and result in zinc contamination of the chamber. The system we used was Denton Vacuum Explorer 14 RF magnetron sputtering system. The sample substrates were 1-inch diameter round fused silica glass to be compatible with the slots on a commercially available filter wheel (shown in Figure 3). The uncoated substrates were solvent-cleaned with acetone, methanol and isopropyl alcohol, and then dried with nitrogen. Then the cleaned sample was placed on the center of stage in the sputtering chamber. The cathode was tilted with respect to the substrate by approximately 20-degrees, but the substrate was rotated during the deposition to provide uniformity of film despite the tilt. The main chamber was then evacuated for about 10 hours to a base pressure below 10^{-6} Torr by a Pfeiffer TMH 261 turbomolecular pump. A 3-minute pre-sputter step was applied with the shutter closed to clean the contamination on the ZnS target surface, and the deposition was performed with an RF discharge power of 100 W in a pure Argon plasma with a working pressure of 8mT. Before each deposition, a calibration was performed to determine the deposition rate. During the calibration process, a silicon substrate with an ink point mark was placed in the sputtering chamber, and the deposition was performed under exactly same conditions as the real substrate. After a certain deposition length, the sample was taken out and the ink point was removed with a lift-off process in a solvent (typically acetone). This produces a bare spot where the underlying substrate is revealed, and the edges of the bare spot are reasonably sharp in order to perform a step height measurement with a stylus profilometer. The film thickness was then measured with the Ambios XP-1 stylus profilometer. With the deposition thickness and the process time, the deposition rate can be precisely calculated. During the subsequently deposition, the substrate of interest is placed in the chamber and the film thicknesses was controlled by manually timing the deposition cycle. The reflection and transmission spectra of the manufactured samples were measured and verified with the Filmetrics F10-VC tool, which is a white light transmission + reflection spectrometer covering the wavelengths from 370 nm to 1050 nm. The six fabricated filters are shown in Figure 3 mounted on two rotating filter wheels for the subsequent multispectral imaging test.

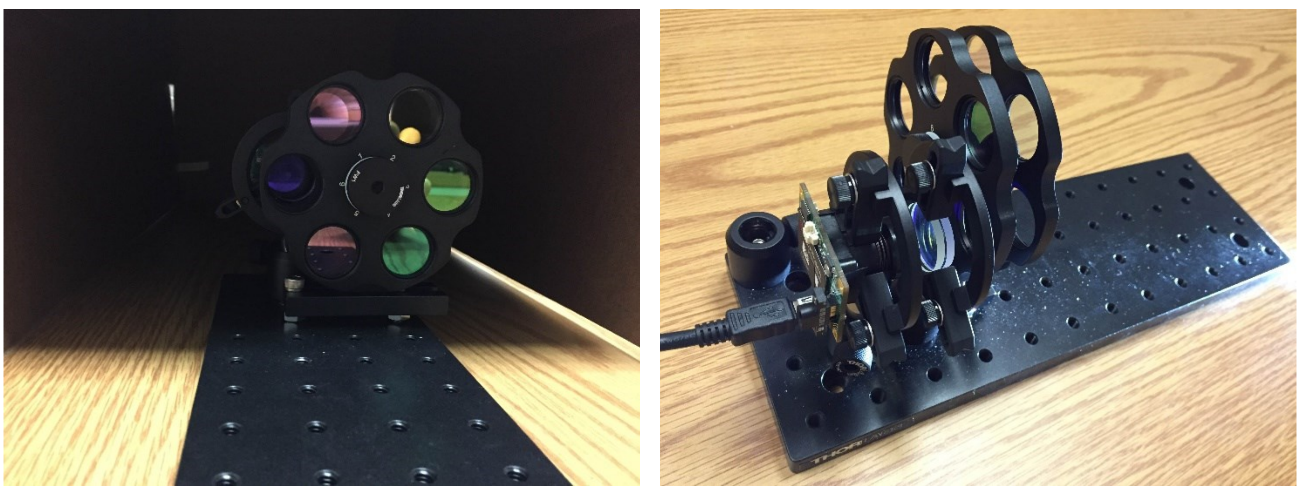

(a) Six manufactured filters mounted on the two filter wheels (b) Multispectral imaging test bed

Figure 3. Manufactured filters and multispectral imaging test bed.

The transmission spectra of all six Fourier spectral filters are shown in Figure 4. The blue line is the ideal sinusoidal transmission with an adjusted contrast and a DC offset; the green line is the design transmission using a transfer matrix method (TMM) analysis; and the red line is the measured transmission.

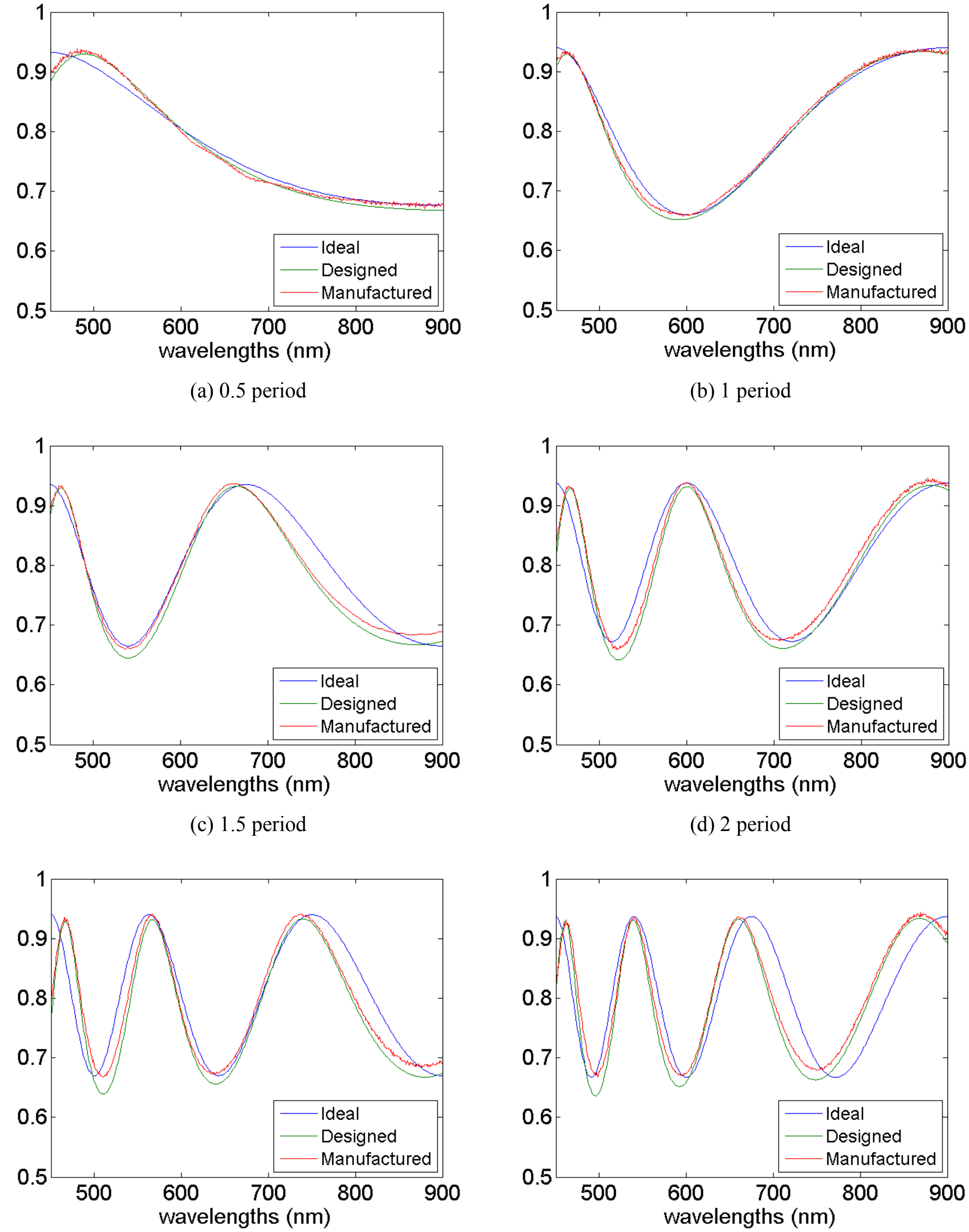

(a) 0.5 period

(b) 1 period

(c) 1.5 period

(d) 2 period

(e) 2.5 period

(f) 3 period

Figure 4. Transmission spectra comparison: the blue lines show the desired ideal sinusoidal transmission function; the green lines are the designed filter spectra that best approximate to ideal function; the red lines are measured transmission spectra from the manufactured filters.

The contrast of the transmission spectrum is around 28%. Although small, this is adequate for our multispectral imaging testbed. There is a small spectral shift between the ideal sinusoid and the design transmission. This is primarily due to the material dispersion. If the material were perfectly free of dispersion, the transmission peaks and valleys would have perfectly matched the ideal sinusoid. The normal dispersion characteristic of most dielectric materials where the indices are larger at shorter wavelength and smaller in longer wavelength will produce a spectra will progressively shrink from the ideal ones. There is also a slightly difference in the transmission amplitude. This is due to the interfaces between different materials (ZnS to fused silica substrate and ZnS to air) in the fabricated filters being not as perfect as in the model. A rough end face would produce some scattering and a reduction in the reflectivity and transmission. Overall, we can verify that the measured spectral shape match very well with the designs and the ideal sinusoid.

3. CONCLUSION

In this paper, we have described the methods used for designing and fabricating the periodic filters based on a Fabry-Perot cavity to approximate the sinusoidal transmittance of the Fourier spectral filters. These designed filters were made using RF sputtering deposition process. The main trade off is between filter contrast and sinusoidal fit. Using ZnS as the cavity material, the measured spectra match very well with the design targets. These filter sets are currently being utilized in a multispectral imaging test bed.

REFERENCES

[1] Lapray, P. J., Wang, X., Thomas, J. B. and Gouton, P., "Multispectral filter arrays: recent advances and practical implementation," Sensors 14(11), 21626-21659 (2014).

[2] Lorente, D., Aleixos, N., Gómez-Sanchis, J., Cubero, S., García-Navarrete, O. L. and Blasco, J., "Recent advances and applications of hyperspectral imaging for fruit and vegetable quality assessment," Food and Bioprocess Technology 5(4), 1121-1142 (2012).

[3] Levenson, R. M., Mansfield, J. R., "Multispectral imaging a review of its technical aspects and applications in anatomic pathology," Veterinary Pathology Online 51(1), 185-210 (2014).

[4] Hirakawa, K. and Barnard, K. J., "Fourier spectral filter array design for multispectral image recovery," OSA Imaging Systems and Applications, Optical Society of America (2014)